

Insulating 3D-printed templates are turned into metallic electrodes: Application as electrodes for glycerol electrooxidation

*Katia-Emiko Guima,^a Victor H. R. Souza,^a Cauê A. Martins^{*ab}*

^aFaculty of Exact Sciences and Technology, Federal University of Grande Dourados, Rodovia Dourados - Itahum, km 12,79804-970, Dourados, MS, Brazil.

^bPhysics Institute, Federal University of Mato Grosso do Sul – Av. Costa e Silva, 79070900, Campo Grande, MS, Brazil

*cauemartins@ufms.br

*Corresponding Author. Phone: +55 67 9 9262-4202

e-mail: cauemartins@ufms.br

Section I: Printing parameters and oxidation states of polyaniline	pg 2
Section II: Electrochemical measurements	pg 2
Section III: Characterization of the electrodes	pg 3
Section IV: Building Pt and Au electrodes on 3D-printed templates: Assessments of activity towards glycerol electrooxidation	pg 4
Section V: Reference	pg 7

Section I: Printing parameters and oxidation states of polyaniline

Table S1. Printing parameters of the electrolyzer

	<i>BT/min</i>	<i>FL/cm</i>	<i>PW/g</i>	<i>MC/US\$</i>
Working electrodes	1	22.9	0.07	0.01

BT = Building time; FL=Filament length; PW=Plastic weight; MC=Material cost.

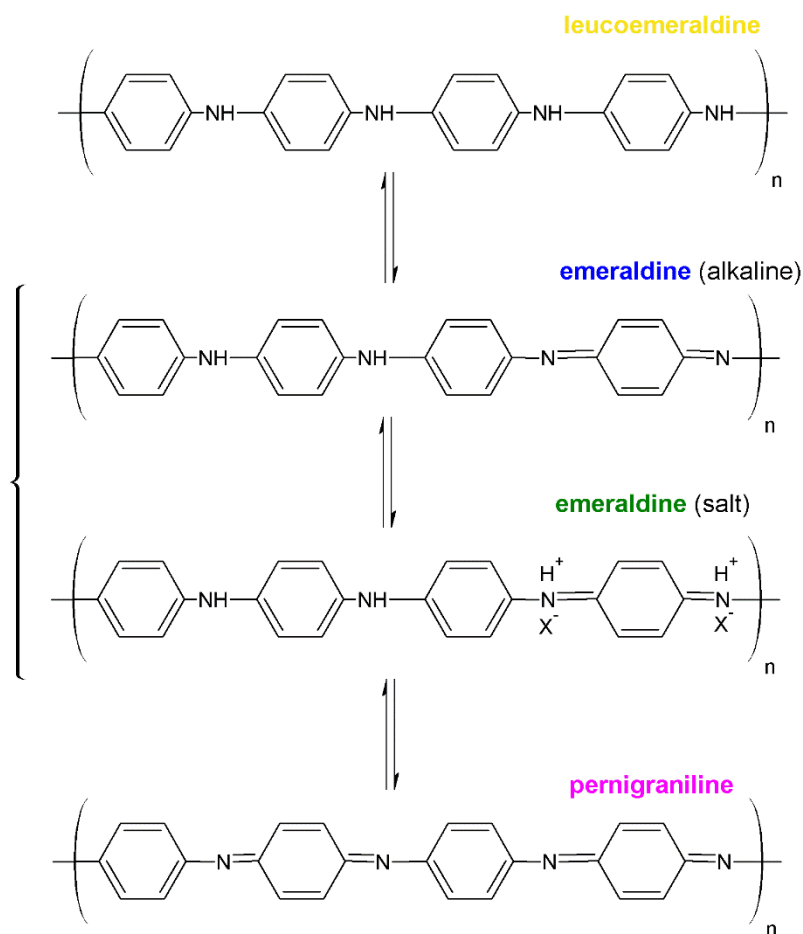


Figure S1. Oxidation states of the polyaniline.

Section II: Electrochemical measurements

Electrochemical measurements were carried out in a potentiostat/galvanostat model μ Autolab Type III with current integrator algorithm. Polymerizations were performed in a 1 mol L⁻¹ HCl supporting electrolyte solution at 0.05 V s⁻¹, as discussed later. H₂PtCl₆·6H₂O, PdCl₂ and HAuCl₄·3H₂O were used as metallic precursors; each

precursor had a concentration of 6 mmol L^{-1} of metal in $0.5 \text{ mol L}^{-1} \text{ H}_2\text{SO}_4$ solution for the electrodeposition process. The electrochemical profiles of Pd, Pt and Au are registered in $0.5 \text{ mol L}^{-1} \text{ H}_2\text{SO}_4$ or $0.1 \text{ mol L}^{-1} \text{ KOH}$, as further indicated in the text. The electrochemically active surface area (ECSA) is calculated considering a specific, well-known charge of a surface reaction on the metals. Namely, (i) for Pt, $210 \mu\text{C cm}^{-2}$ is considered as the charge involved in the desorption of a hydrogen monolayer; (ii) for Pd, $420 \mu\text{C cm}^{-2}$ is considered as the charge released by the desorption of a Pd oxide monolayer; and (iii) for Au, $386 \mu\text{C cm}^{-2}$ as the charge involved in the reduction of a Au oxide monolayer. All electrodes were used as catalysts for glycerol electrooxidation in an alkaline medium. Electrochemical measurements were performed using an Ag/AgCl as reference electrode, except for the electrochemical growth of PANI, which was performed using a reversible hydrogen electrode (RHE). All potentials are corrected to RHE scale. A high-surface-area Pt plate was used as counter electrode. The potential ranges for registering electrochemical profiles and to perform glycerol electrooxidation are found through the text.

Section III: Characterization of the electrodes

Scanning electron microscopy (SEM) images were acquired with an FEG/SEM (Tescan) by using an electron beam of 10 kV. All images were registered using an in-beam secondary electron detector. Energy dispersive spectroscopy (EDS) analysis of the modified electrodes was performed with a coupled EDS detector (Oxford Instruments). The elemental analyses were carried out using a mapping mode from the area of each selected image

Section IV: Building Pt and Au electrodes on 3D-printed templates: Assessments of activity towards glycerol electrooxidation

The most common catalyst for the electrooxidation of glycerol and other alcohols electrooxidation is Pt. Taking this into consideration, we also built an indirect-3D-printed Pt electrode. The same protocol was followed to turn the PLA onto a GR/PAni/PLA template. Afterwards, the template was immersed in a $6 \text{ mmol L}^{-1} \text{ H}_2\text{PtCl}_6 \cdot 6\text{H}_2\text{O}$ in $0.5 \text{ mol L}^{-1} \text{ H}_2\text{SO}_4$ for potentiodynamic electrodeposition between 0.05 and 1.2 V. Similar to the previous case, the currents associated with the surface phenomena become more evident as more Pt is deposited on the template, as shown by the H_{UPD} region in Figure S2A. After the electrodeposition process, a profile was registered to guarantee a successful Pt partial covering (Figure S2B).

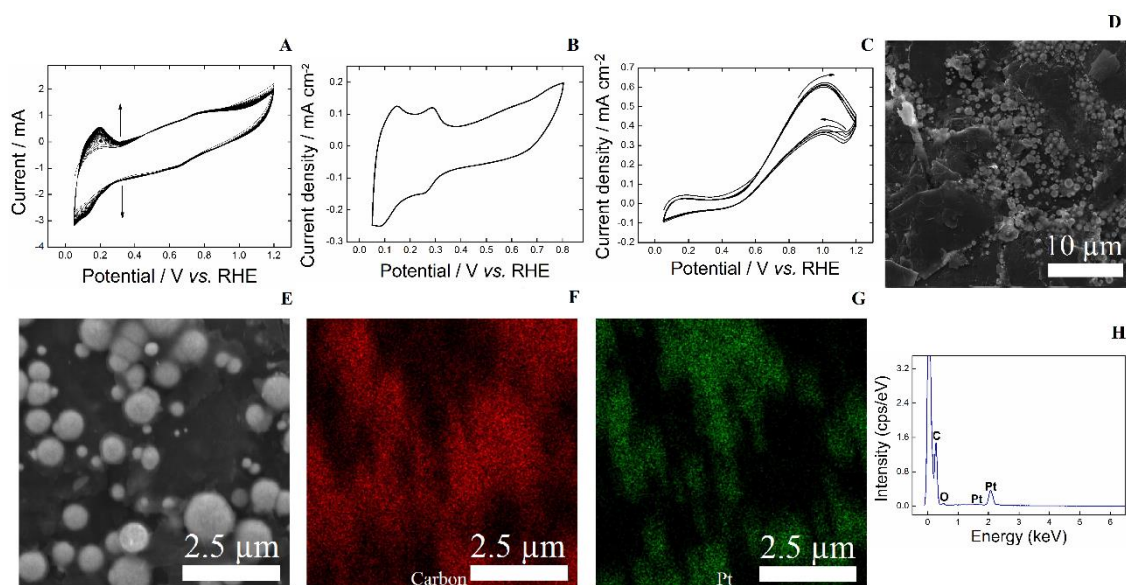


Figure S2.(A) Potentiodynamic electrodeposition process achieved by successive potential cycles of GR/PAni/PLA template in $6 \text{ mmol L}^{-1} \text{ H}_2\text{PtCl}_6 \cdot 6\text{H}_2\text{O}$ in $0.5 \text{ mol L}^{-1} \text{ H}_2\text{SO}_4$ between 0.05 and 1.2 V. (B) Cyclic voltammogram of the indirect-3D-printed Pt electrode in $0.5 \text{ mol L}^{-1} \text{ H}_2\text{SO}_4$ between 0.05 and 0.8 V. (C) Cyclic voltammograms in the presence of 0.2 mol L^{-1} glycerol + 0.1 mol L^{-1} KOH between 0.05 and 1.2 V. All measurements were performed at 0.05 V s^{-1} . (D) and (E) show representative SEM images, while

(F) and (G) show EDS K α elemental composition maps (indicated in the Figure). (H) EDS spectrum of the indirect-3D-printed Pt electrode.

Figure S2B shows a characteristic profile of a Pt electrode in 0.5 mol L⁻¹ H₂SO₄. The H_{UPD} region is evident between 0.05 and 0.35 V; however, the profile is slightly inclined, suggesting resistivity to some extent. This feature may be a consequence of a large region absence of metal deposition, compared to the Pd electrode, which does not affect the catalytic properties, as seen in Figure S2C.

The electroactivity of the Pt electrode was investigated in 0.2 mol L⁻¹ glycerol + 0.1 mol L⁻¹ KOH in the range of 0.05-1.2 V. Five successive cyclic voltammograms are shown in Figure S2C, displaying anodic currents during the positive and negative potential sweep, both centered at ~1.0 V. The onset potential is 0.44 V, which is lower than that of the same reaction in acid medium (0.6-0.7 V). This shift towards lower potentials in alkaline medium is a consequence of the application of the Nernst equation, from which it is evident that electrooxidation is benefited in alkaline medium while electroreduction is facilitated in acid medium. This result is similar to those found by Gomes *et al.*¹ They found ~0.5 V as onset potential and 0.95 V as peak potential for glycerol electrooxidation (0.1 mol L⁻¹ glycerol + 0.1 mol L⁻¹ NaOH) on bulk Pt.¹

Figures S2D and S2E show representative SEM images of the indirect-3D-printed Pt electrode. The Pt particles are well-shaped, delineating clear spheres ranging from 100 nm to 1.5 μ m. The non-uniform size distribution may be a consequence of potentiodynamic electrodeposition, where nanoparticles may act as a center of nucleation to build further clusters. The main achievement of this work is that the Pt was successfully deposited on the template, as shown by the EDS mapping composition in the region of carbon (Figure S2F) and in the Pt region (Figure S2G). Moreover, the EDS spectrum of

the indirect-3D-printed Pt electrode shown in Figure S2H assures the presence of Pt through the peak at ~ 2.06 keV.

Another potential candidate to be used as catalyst in alcohol fuel cells and electrolyzers in alkaline medium is Au. An indirect-3D-printed Au electrode was built by following the same protocol as those aforementioned. Successive potential cycles in the range of 0.05-1.75 V were applied to the GR/PAni/PLA template in the presence of $6 \text{ mmol L}^{-1} \text{ H AuCl}_4 \cdot 3\text{H}_2\text{O}$ in $0.5 \text{ mol L}^{-1} \text{ H}_2\text{SO}_4$, as shown in Figure S3A. The increase peak currents in two regions of the voltammogram shows the electrodeposition of Au; one between 1.2 and 1.75 V at the positive scan related to the gold surface oxides and that between 1.4-0.8 V during the reverse scan related to the reduction of surface oxides. The characteristic Au profile shown in Figure S3B was obtained in $0.1 \text{ mol L}^{-1} \text{ KOH}$ between 0.05 and 1.65 V. The activity of the Au electrode was also investigated for glycerol electrooxidation, as shown in Figure S3C. Similar to what occurs for glycerol electrooxidation on Pd and Pt, the alcohol is electrooxidized during the direct and reverse potential scans. The onset potential is 0.7 V, afterwards, the anodic current increases until it reaches a maximum value at ~ 1.28 V, and then decreases for more positive potentials. These electrocatalytic parameters are similar to those reported for glycerol electrooxidation (0.1 mol L^{-1} glycerol + 0.1 mol L^{-1} NaOH) on bulk Au.¹ Gomes *et al.* found 0.65 V and ~ 1.4 V as onset and peak potential, respectively.¹

During the reverse scan, the surface is reactivated and starts oxidizing the alcohol and the partially oxidized compounds at ~ 1.2 V, forming a well-defined peak centered at 1.15 V.

Figure S3D shows a representative SEM image of the Au electrode. The potentiodynamic electrodeposition leads to the growth of non-uniform polygonal-shaped

Au particles having diameters of about 200-700 nm. A section of another region of the electrode surface (Figure S3E) was also investigated by EDS compositional mapping. Figure S3F shows an extended red-colored region dominated by carbon species, whereas the Au particles are shown by the green-colored regions in Figure S3G. Finally, the EDS spectrum from Figure S3H indicates the presence of Au through the peak at ~ 2.15 keV.

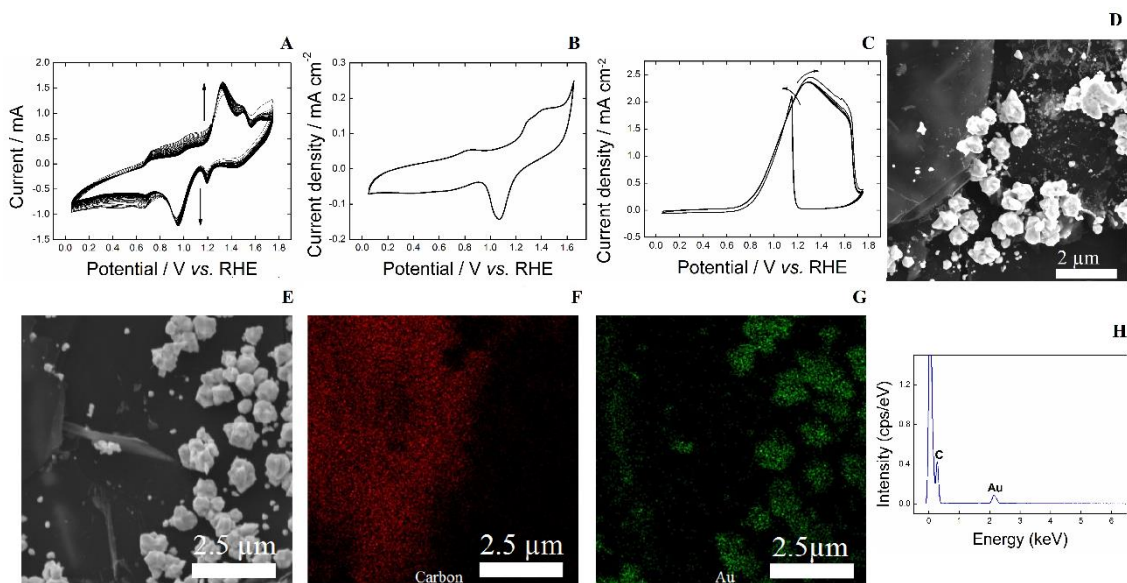


Figure 5. (A) Potentiodynamic electrodeposition process achieved by successive potential cycles of GR/PAni/PLA template in $6 \text{ mmol L}^{-1} \text{ HAuCl}_4 \cdot 3\text{H}_2\text{O}$ in $0.5 \text{ mol L}^{-1} \text{ H}_2\text{SO}_4$ between 0.05 and 1.75 V. (B) Cyclic voltammogram of the indirect-3D-printed Au electrode in $0.1 \text{ mol L}^{-1} \text{ KOH}$ between 0.05 and 1.65 V and (C) in the presence of 0.2 mol L^{-1} glycerol between 0.05 and 1.75 V. All measurements performed at 0.05 V s^{-1} . (D) and (E) show representative SEM images, while (F) and (G) show EDS K α elemental composition maps (indicated in the Figure). (H) EDS spectrum of the indirect-3D-printed Au electrode.

Section V: Reference

1J. F. Gomes and G. Tremiliosi-Filho, *Electrocatalysis*, 2011, **2**, 96.